

## **The design for the LCLS rf photo-injector\***

R. Alley, V. Bharadwaj, J. Clendenin, P. Emma, A. Fisher, J. Frisch, T. Kotseroglou\*, R. Miller, D. T. Palmer, J. Schmerge, J. C. Sheppard, M. Woodley, A. D. Yeremian  
*Stanford Linear Accelerator Center, Stanford University, Stanford, CA 94309*

J. Rosenzweig  
*University of California, Los Angeles, CA*

D.D. Meyerhofer  
*Dept. of Physics and Astronomy, Dept. of Mechanical Engineering, University of Rochester, Rochester, NY 14627*

L. Serafini  
*INFN, University of Milan, Milan, Italy*

**Presented at**

**20TH INTERNATIONAL FREE ELECTRON LASER AND 5TH FREE  
ELECTRON LASER USERS' WORKSHOP (FEL 98)**

**16-21 Aug 1998 , Williamsburg, VA:**

---

\* Work supported by Department of Energy contract DE-AC03-76SF00515.

♣ Corresponding author, e-mail: theo@slac.stanford.edu.

# The design for the LCLS rf photo-injector\*

*R. Alley, V. Bharadwaj, J. Clendenin, P. Emma, A. Fisher, J. Frisch, T. Kotseroglou\*, R.*

*Miller, D. T. Palmer, J. Schmerge, J. C. Sheppard, M. Woodley, A. D. Yeremian*

Stanford Linear Accelerator Center, Stanford University, Stanford, CA 94309

*J. Rosenzweig*

University of California, Los Angeles, CA

*D.D. Meyerhofer*

Dept. of Physics and Astronomy, Dept. of Mechanical Engineering, University of

Rochester, Rochester, NY 14627

*L. Serafini*

INFN, University of Milan, Milan, Italy

## Abstract

We report on the design of the rf photoinjector of the Linac Coherent Light Source (LCLS). The rf photoinjector is required to produce a single 150 MeV bunch of  $\sim 1$  nC and  $\sim 100$  A peak current at a repetition rate of 120 Hz with a normalized rms transverse emittance of  $\sim 1 \pi$  mm-mrad. The design employs a 1.6-cell S-band rf gun with an optical spot size at the cathode of a radius of  $\sim 1$  mm and a pulse duration with an rms sigma of  $\sim 3$  ps. The peak rf field at the cathode is 150 MV/m with extraction  $57^\circ$  ahead of the rf peak. A solenoidal field near the cathode allows the compensation of the initial emittance growth by the end of the injection linac. Spatial and temporal shaping of the laser pulse striking the cathode will reduce the compensated emittance even further. Also, to minimize the contribution of the thermal emittance from the cathode surface, while at the same time optimizing the quantum efficiency (QE), the laser wavelength for a Cu cathode should be tunable around 260 nm. Following the injection linac the geometric emittance simply damps linearly with energy growth. PARMELA simulations show that this design will produce the desired normalized emittance, which is about a factor of two lower than has been achieved to date in other systems. In addition to low emittance, we also aim for laser amplitude stability 1% in the UV and a timing jitter in the electron beam of 0.5 ps rms, which will lead to less than 10% beam intensity fluctuation after the electron bunch is compressed in the main linac.

---

\* Work supported by Department of Energy contract DE-AC03-76SF00515.

♣ Corresponding author, e-mail: theo@slac.stanford.edu.

## 1. Introduction

The LCLS [1] is a future free electron laser (FEL) in the 1-Angstrom wavelength regime, in which a low emittance electron beam is generated with an rf photoinjector, accelerated to 15 GeV using existing sectors of the SLAC 3-km linac and compressed at intermediate energies by two magnetic chicanes to a length of 20  $\mu\text{m}$ . Subsequently, the beam is injected into 100 m of undulator. FEL lasing is produced in a single pass of the electron beam through the undulator by Self-Amplified-Spontaneous-Emission (SASE).

The electron source for the LCLS consists of a high-gradient 1.6-cell S-band rf gun with a copper photocathode illuminated by intense optical pulses at 260 nm provided by a Nd:YAG-pumped Ti:Sapphire laser system whose fundamental frequency is tripled. The source must produce a nominal 1 nC pulse with low transverse and longitudinal emittance at a pulse repetition rate of 120 Hz. The required  $1\sigma$  rms emittance for the nominal charge is  $< 1\pi$  mm-mrad. A significant part of the overall emittance produced by the source is expected to be contained in the spatial and temporal halo of the pulse, which can be removed downstream of the photoinjector, if desired, with scrapers. To meet the emittance requirements, the optical spot size at the cathode has a radius of  $\sim 1$  mm, the pulse duration has an rms sigma of  $\sim 3$  ps, and the rf field at the cathode is 130-150 MV/m.

## 2. RF Photocathode gun

The rf gun design is based on the 1.6-cell gun developed by a BNL/SLAC/UCLA collaboration [2]. The parameters of the gun as applied to the LCLS are listed in **Table 1**. To minimize emittance growth due to the  $E_z$  component of the TM<sub>110</sub> mode, the gun has been symmetrized. The original BNL zero-mode-suppressed side coupling has been replaced by side-coupling rf into the full cell only. In consequence the cell-to-cell coupling between the two cells has been improved by increasing the iris size, which also increases the mode separation between the zero and  $\pi$ -modes. This arrangement allows for more precise field balancing during tuning. To provide more rf focusing and decrease the peak field on the cell-to-cell iris, the half-cell length has been slightly increased.

A schematic of the gun is shown in **Fig.1**. There are two identical coupling ports in the full cell, located  $180^\circ$  apart. The rf waveguide is connected to one port and a vacuum pump to the second. For diagnostic purposes, an rf monitoring loop is also located in the second port. The photocathode is located at the geometric center of the end-plate of the half-cell. The end-plate is removable to facilitate installation of cathode material other than Cu by implantation or by using an insert. The laser beam can be brought to the cathode either along the axis of the gun or at grazing incidence through the  $72^\circ$  side port (not shown in the figure). The peak electric field at the cathode is 150 MV/m and the laser pulse is injected  $57^\circ$  ahead of the peak.

The 15 MW in rf power required for the gun will be provided by the first of the two klystron stations in Linac 0, the first accelerator section after the rf gun and up to a chicane (See Section 5.). Phase and amplitude for the gun can be set independently of the downstream injector accelerating sections. A diagnostic section of 0.75 m will separate the exit of the gun from the entrance of Linac 0. Apart from including vacuum isolation valves, this drift space will contain a beam position monitor (BPM), current monitor, Faraday cup, profile screen, and steering magnets.

## 3. Photocathode

A metal photocathode is chosen for the rf gun. The QE for Cu illuminated with UV light depends somewhat on surface preparation, but a QE of  $10^{-5}$  at 260 nm seems reasonably conservative for normal incidence

[3,4,5]. A gain in QE by a factor of two to four can be achieved by illuminating the cathode at a grazing angle. At 260 nm an optical pulse of  $\sim 500 \mu\text{J}$  on the cathode is required to produce 1 nC of charge when the QE is  $10^{-5}$ .

The principal advantage of a metal cathode is that its QE is relatively impervious to exposure to atmospheric air or the vacuum environment of the operating gun. Thus special cathode preparation and installation (e.g. load-lock) techniques are less critical.

The photoelectric response of metal cathodes is on the sub-picosecond level, thus imposing no limitation on any desired temporal pulse shaping. Finally, the use of Cu as the cathode allows the entire end plate of the half cell to be formed in the standard manner of Cu rf cavities, permitting operation at the highest field values. The use of a cathode plug or insert in an S-band gun has so far limited the cathode field to about 80 MeV/m, whereas simulations indicate the transverse emittance drops with increasing field up to about 140 MeV/m. Nonetheless, since the QE of Mg cathodes is several times higher than for Cu, we are searching for a way to use a Mg cathode with fields on the order of 150 MV/m.

## 4. Laser

The laser system [6] is required to deliver a  $500 \mu\text{J}$  pulse of UV photons to the cathode at a repetition rate of 120 Hz. To meet the emittance requirements of the source, the laser must have a pulse length in the range of 3-5 ps rms and radius of  $\sim 1$  mm hard edge on the cathode in order to balance the effects of space charge and rf on emittance growth in the gun itself. Pulse shaping is required to optimize both the transverse and longitudinal emittance. Stability of the laser pulses of better than 0.5 ps rms in time and 1% in energy in the UV is crucial for the bunch compressors and FEL. The laser system is shown in **Fig. 2**. A CW, frequency doubled, diode pumped Nd:YAG laser provides energy in the green (532 nm) to pump the CW mode-locked Ti:Sapphire oscillator, which delivers a continuous train of 10 nJ, 100 fs FWHM pulses that repeat at 119 MHz. By using this frequency, which is the 24<sup>th</sup> sub-harmonic of the linac's 2856 MHz rf, the timing of the laser pulse can be locked to the phase of the rf in the linac and gun. The timing system is shown in **Fig. 3** and described in more detail in ref. [1]. The wavelength of the oscillator is tuned to 780 nm, which after amplification is frequency tripled to 260 nm. With the possible exception of a timing stability of 0.5 ps rms, oscillators of this type are commercially available. A Pockels cell and polarizer are used to gate single pulses, at 120 Hz, from the 119 MHz pulsetrain. The selected pulses are then amplified by two multipass Ti:Sapphire crystals, both configured as 4-pass "bow-tie" amplifiers. Both are pumped by a single Q-switched, doubled Nd:YAG laser that can produce a 120 Hz train of 3 ns pulses, which is also a commercial system. The pump output is stabilized by "trimming" a few percent of the main pump pulse by the use of a Pockels cell.

The system uses chirped pulse amplification (CPA) [7] to avoid damage and nonlinearities in the amplifiers. The large bandwidth of Ti:Sapphire enables us to use pulse shaping in time at the 0.1 ps level in order to optimize the emittance of the electron beam in the gun and injector. This is done by a computer controlled Liquid Crystal Display (LCD) mask, which is positioned in the Fourier plane of two gratings just after the oscillator.

After the second amplifier, the transverse shape of the pulse is modified from Gaussian to uniform to better match the requirements for obtaining a low emittance from the gun. The laser pulse is then tripled in frequency and transported to the gun by means of Fourier imaging that also includes compensation for the temporal and spatial distortion caused by grazing incidence onto the photocathode.

The energy management of the system is as follows: transmission through the spatial flattener  $\sim 50\%$ , through the compressor  $\sim 50\%$ , through the tripling stage  $\sim 25\%$  and through the optical transport to the gun  $\sim 50\%$ . Consequently starting from 18 mJ in the IR after the second amplifier, the required  $500 \mu\text{J}$  of UV is delivered to the cathode. Table 2 is a summary of the laser parameters.

## 5. Linac 0.

The design of Linac 0 was originally described in ref. [8]. Some additional details can be found in ref. [1]. Linac 0 consists of four SLAC-type 3m S-band accelerator sections, associated solenoid, and necessary drift sections with diagnostics. It is preceded by the rf gun and diagnostic section and followed by a second diagnostic section and an achromatic bend system (low energy dog-leg) that brings the beam into the 15 GeV linac. The layout of the photoinjector system is shown in **Fig. 4**. The overall length from the photocathode to the last accelerator section output flange is 15.8 m, including four drift sections of 75, 47, 105 and 105 cm respectively. The gun solenoid is 20 cm in length and is located 19.8 cm downstream of the photocathode. Two linac solenoids, each 70 cm in length are located at the end of accelerating sections 2 and 3 respectively.

Two SLAC-type 5045 klystrons are required, one to power the gun and the first two 3 m sections and the other for the last two 3 m sections. They will be operated in an un-SLEDeD mode [9]. As shown in **Fig. 4** high power rf phase shifters and attenuators will allow the independent control of the gun and first two 3 m sections.

In Linac 0, after each accelerator section there will be a Beam Position Monitor (BPM), a current monitor, and a screen. Between the second and third sections, an X-band cavity will be placed alongside a ceramic gap in the beamline. The charge-normalized rf intensity generated in this cavity as an electron bunch passes through, can be used to minimize the bunchlength. Transverse emittance diagnostics are included in the dog-leg system.

## 6. Emittance compensation

In 1989 Carlsten [10] pointed out that by simply placing a solenoidal field at the proper location at the gun one can reverse the evolution of phase space such that at a latter point downstream the individual phase spaces of the various slices of the beam will momentarily be aligned. Emittance compensation in the rf gun is done by using a solenoid with precisely defined field symmetry and positioned at the gun's exit to an accuracy of 25  $\mu\text{m}$ . An identical compensation magnet with current flow in the opposite sense will be used to null the magnetic field at the cathode. We base our design on recent experiments at the ATF at BNL [11] that have shown encouraging results on emittance compensation, as shown in **Fig. 5**.

Emittance compensation in Linac 0 was studied extensively using PARMELA as originally described in ref. [8]. In the first 3-m section, where the gradient is 7 MV/m, a 1.5% energy spread for the full beam is introduced to help in emittance compensation by placing the centroid of the beam  $\sim 5^{\circ}$  ahead of the rf crest. This energy spread is removed in the last two 3 m sections, where the gradient is 17 MeV/m, by placing the rf such that the beam is slightly behind the crest. The magnetic field in the emittance compensation solenoid at the gun is slightly less than 3 kG with an effective length of  $\sim 20$  cm, while the solenoid between the accelerating sections is slightly greater than 3 kG with an effective length of 70 cm.

At the entrance to the third 3-m section, the beam energy is  $\sim 50$  MeV so that space charge effects are much reduced. The rf field gradient though, is more than double in this section as in the previous two, so the beam radius is purposely reduced by using a solenoid between the second and third sections. The transverse space charge distribution at the cathode is assumed to be uniform and the temporal shape Gaussian with an rms sigma of 4.4 ps, truncated at  $\pm 2$  sigma, resulting in overall rms length of 3.8 ps. **Table 3** and **Figures 6** and **7** show the resulting electron beam parameters at the end of Linac 0.

## 7. Summary

We have presented the design of the rf photoinjector of the Linac Coherent Light Source (LCLS). The rf photoinjector is required to produce a single 150 MeV bunch of  $\sim 1\text{nC}$  and  $\sim 100$  A peak current at a repetition rate of 120 Hz with a normalized rms transverse emittance of  $\sim 1\pi$  mm-mrad. The design employs a copper cathode, 1.6-cell S-band rf gun, which has been symmetrized, a CPA, Ti:Sapphire laser system that is pulse-shaped, frequency tripled and stabilized both in timing and intensity and a linac 0 with 4 3-m

SLAC type accelerating sections. PARMELA simulations show that this design will produce a beam with the desired characteristics at 150 MeV.

## References

- [1] LCLS Design Study Report, SLAC-R-521, UC-414, April 1998.
- [2] D.T. Palmer et al., SPIE 2522 (1995) 514.
- [3] T. Srinivasan-Rao et al. J. Appl. Phys. 69 (1991) 3291.
- [4] P. Davis et al., Proc. of the 1993 Particle Accelerator Conference, p.2976.
- [5] E. Chevallay et al., Nucl. Instrum. and Meth. A 340 (1994) 146.
- [6] T. Kotseroglou et al., The LCLS source laser, SLAC-PUB-7755, paper presented at the Int'l Conf. on Lasers '97, New Orleans, LA, Dec. 15-19, 1997.
- [7] P. Maine et al., IEEE J. Quantum Electron. QE-24 (1988) 398.
- [8] A. D. Yeremian, et. al., "Proposed injector for the LCLS Linac", IEEE Proceedings of the Particle Accelerator Conference, vol 3, p. 2855, Vancouver BC, 1997.
- [9] Z.D. Farkas et al., "SLED: A Method of Doubling SLAC's Energy", Proceedings, 9th Int. Conference on High Energy Accelerators, SLAC, CA, May 2-7, 1974, p.576 and SLAC-PUB-1453.
- [10] B.E. Carlsten, Nucl. Instrum. and Meth. A 285 (1989) 313.
- [11] D.T. Palmer et al., 'Experimental Results of a single Emittance Compensation Solenoidal Magnet', SLAC-PUB-7421, (May 1997), presented at the 17<sup>th</sup> IEEE Particle Accelerator Conference, Vancouver, B.C., Canada, May 12- 16, 1997.

## FIGURES AND TABLES

**Table 1.** Photoinjector gun parameters. A uniform temporal laser pulse profile is assumed.

Parameter	Value
Cathode material	Cu (or possibly Mg)
Usable diameter of cathode	12 mm
Quantum efficiency	$10^{-5}$ at 260 nm
Nominal extraction field	140 MV/m
Charge per bunch	~1nC
Peak current	~100 A
Beam energy at gun exit	7 MeV
Energy spread at exit	0.2% rms
RF frequency	2856 MHz
Bunch rep rate	120 Hz
RF pulse duration	3-4 $\mu$ s
RF peak power	15 MW
Number of cells	1.6
Length	0.168 m

**Table 2.** Laser system requirements.

<b>Parameter</b>	<b>Value</b>
Operating wavelength	260-280 nm
Pulse rep rate	120 Hz
Number of micropulse per pulse	1 (for LCLS-I), 40 (for LCLS-II)
Pulse energy on cathode	>500 $\mu$ J
Pulse radius on cathode	$\sim$ 1mm HWHM
Pulse risetime	1.0 ps
Pulse length	10 ps ( tunable)
Longitudinal pulse form	Various
Transverse pulse form	Uniform
Homogeneity on cathode	10% ptp
Pulse to pulse energy jitter	< 1%
Laser to rf stability	< 0.5 ps rms
Spot diameter jitter on cathode	1% ptp
Pointing stability	< 1% ptp

**Table 3.** Electron beam parameters at end of Linac 0. Ref. [8].

<b>Parameter</b>	<b>Value</b>
Energy	150.5 MeV
Bunch charge	1.0 nC
rms pulse length	2.3(0.69) ps(mm)
Halo population	7.7%
rms relative energy spread	0.13%
Normalized rms core emittance	1.1 $\pi$ mm-mrad

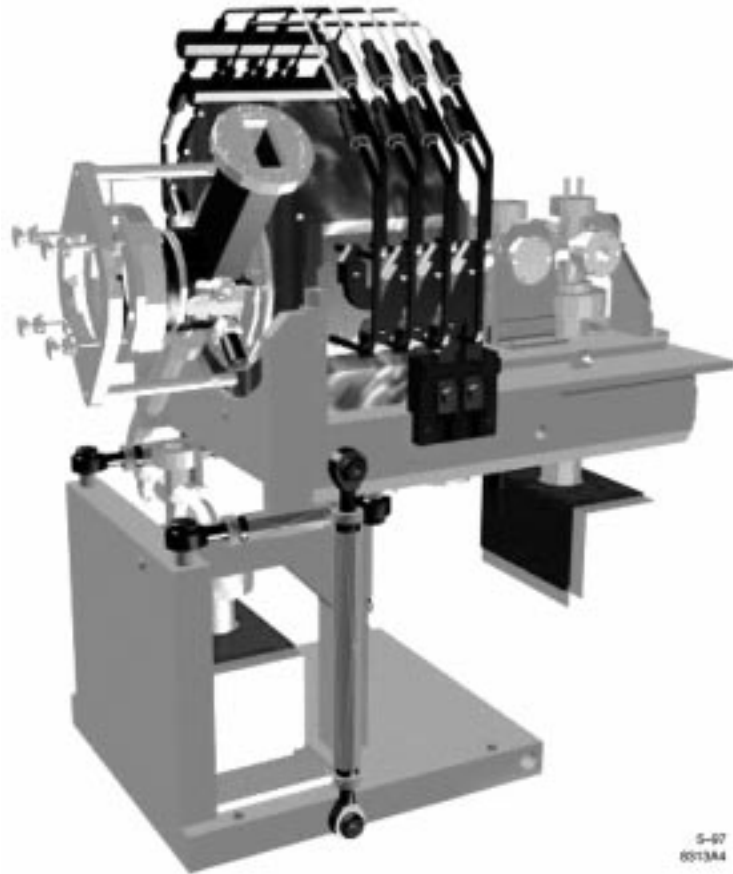
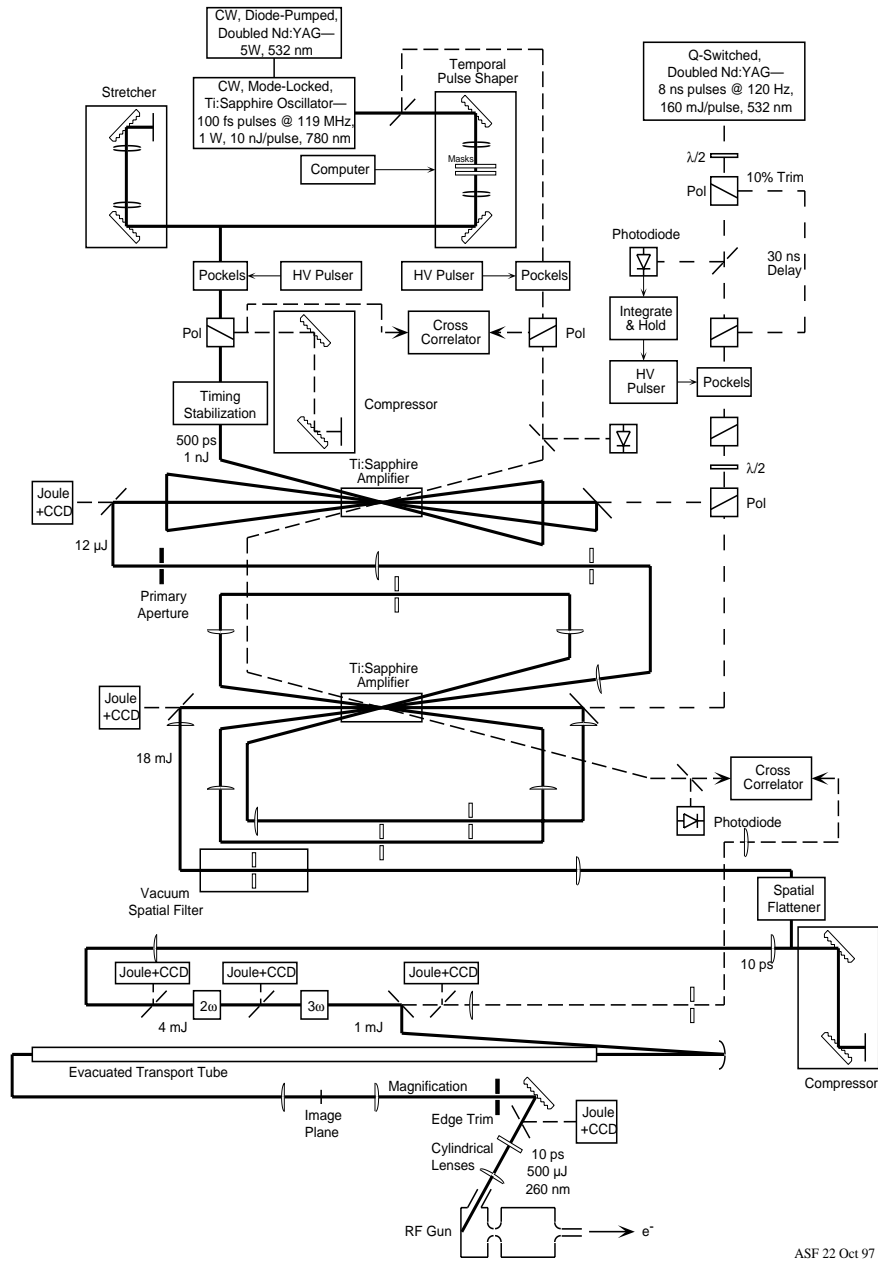


**Figure 1.** Perspective of the gun assembly. The beam exits to the right. ( Figure by C. Stelmach and S. Pjerov, NSLS, BNL).



ASF 22 Oct 97

**Figure 2.** The drive laser for the rf photocathode electron gun for the LCLS. The thick lines show the main beam path, the closely spaced, dashed lines indicate diagnostic beams, and the widely spaced, dashed lines are pump beams.

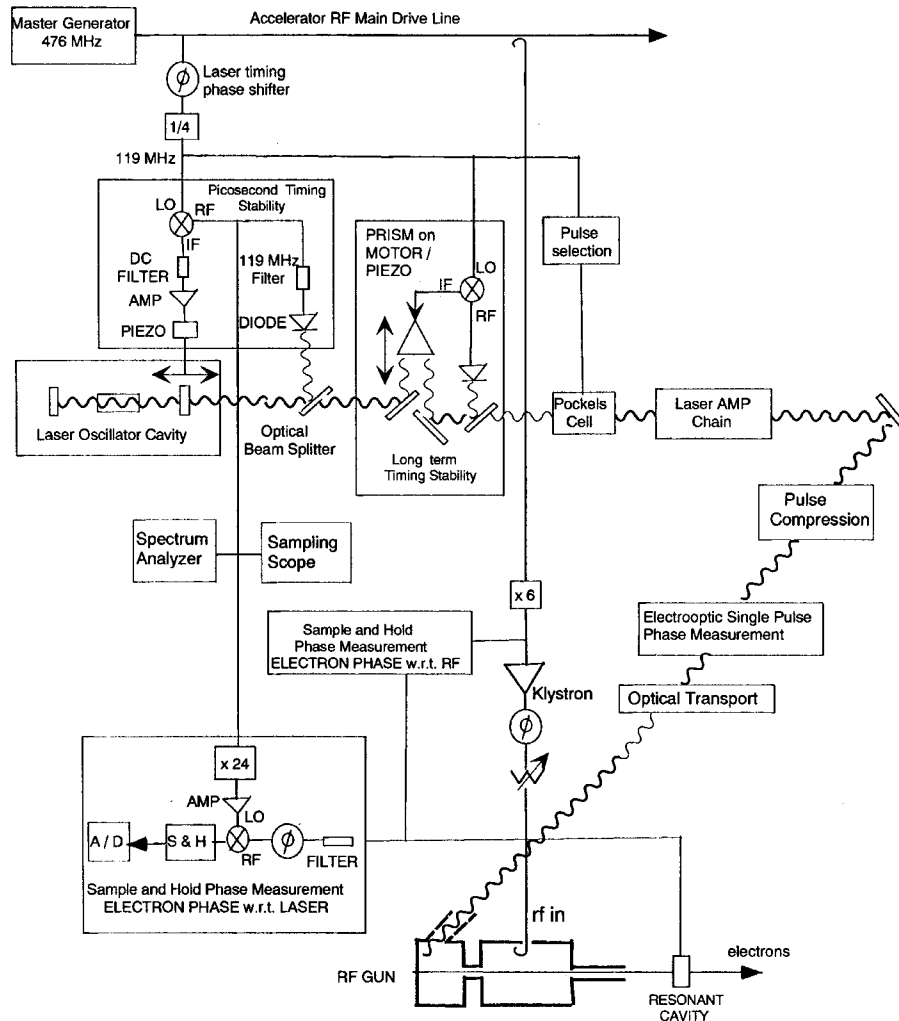
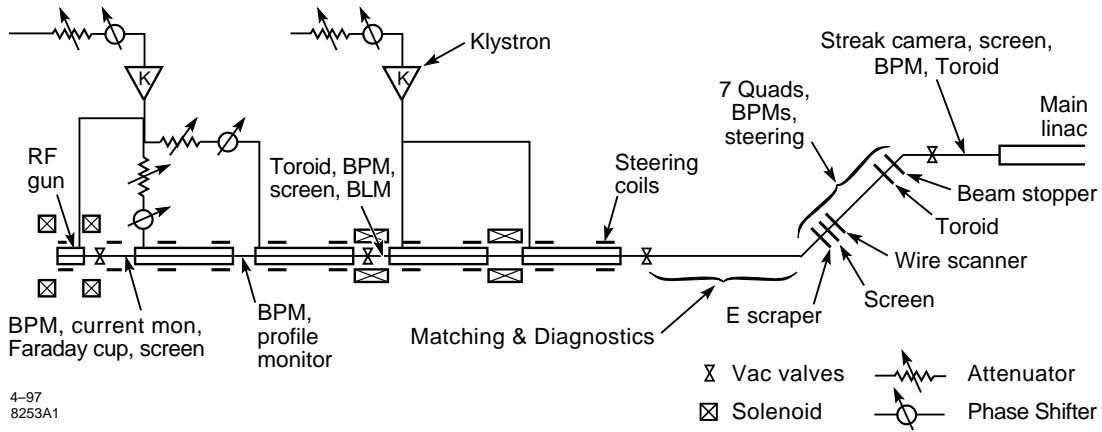
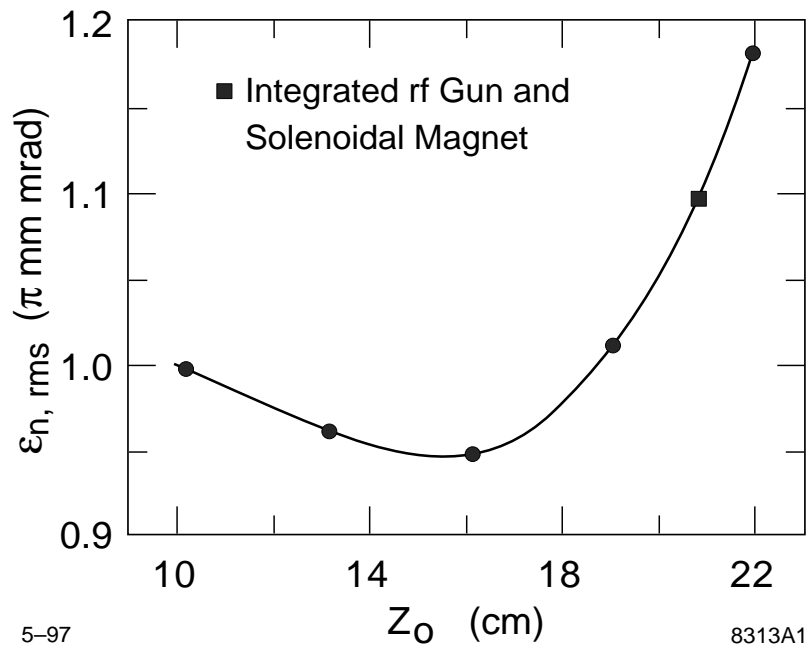


Figure 6.1-6

**Figure 3.** Timing stabilization scheme. The laser oscillator cavity length is stabilized by the use of a piezo on the cavity end mirror. An external optical delay line corrects for slow drifts of the phase of the laser w.r.t. the electrons produced.



**Figure 4.** Overall layout of the LCLS photoinjector showing the rf gun, Linac 0, and the low-energy dog-leg, with drift sections and diagnostics indicated. Ref. [8].



**Figure 5.** PARMELA simulation of compensated normalized emittance of ATF gun and beamline as a function of position (defined as the center) of the emittance compensating solenoid. The actual position of the solenoid during the experiments is shown by the square data point.

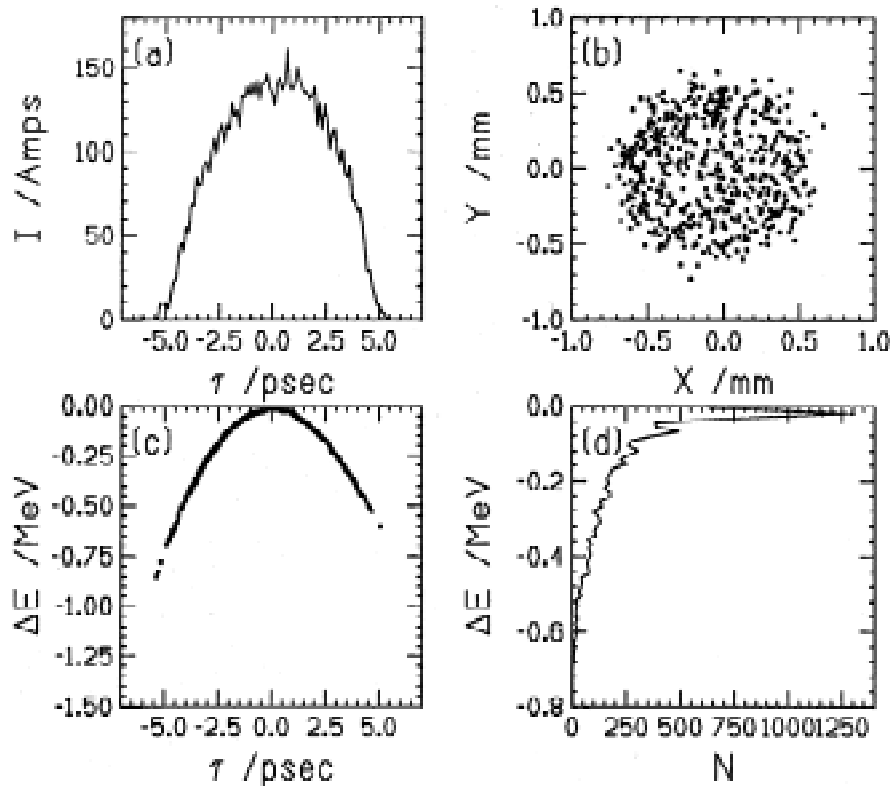


**Figure 6.** PARMELA results for bunch at 150 MeV showing: (top left) temporal distribution; (top right) x-y space; (bottom left) longitudinal phase space; and (bottom right) energy distribution. Ref. [8].

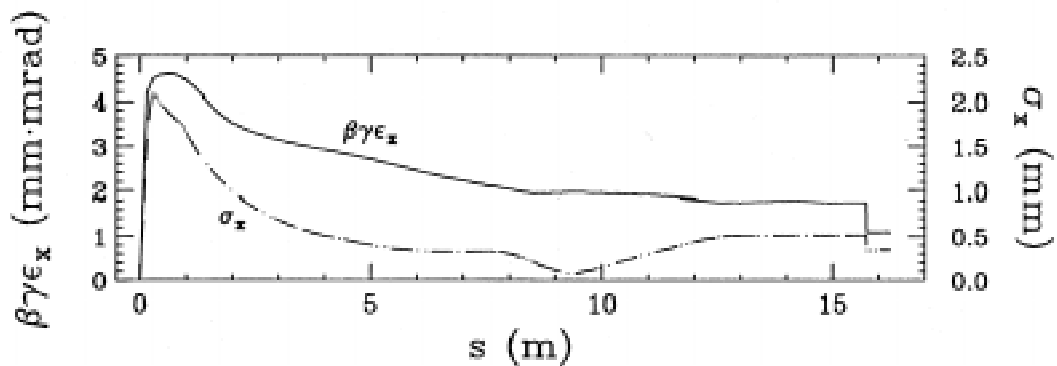


**Figure 7.** Normalized emittance ( solid line) and rms beam size ( dashed line) along the beamline from the cathode ( $s=0$ ) to 150 MeV at the end of Linac 0. The step at  $s \sim 16$  m is a 7.7% halo cut ( in simulation only). Ref. [8].